Speckle-Visibility Spectroscopy of Depolarized Dynamic Light Scattering

David Bossert[a], Jens Natterodt[a], Dominic A. Urban[a], Christoph Weder[a], Alke Petri-Fink[a,b], and Sandor Balog[a]*

[a] Adolphe Merkle Institute, University of Fribourg, Chemin des Verdiers 4, 1700 Fribourg, Switzerland

[b] Chemistry Department, University of Fribourg, Chemin du Musée 9, 1700 Fribourg, Switzerland

*Corresponding author: sandor.balog@unifr.ch

Supporting Information

Table of Contents

Dynamic Depolarized Light Scattering and Particle Systems

DDLS has been used to characterize rod- and ellipsoid-like particles,[1-9] cellulose whiskers,[10] carbon nanotubes,[11-15] liquid crystals,[16-17] particles supporting localized surface plasmon resonances,[18-24] rotationally asymmetric and Janus particles,[25-28] aggregates, agglomerates and clusters resulting from particle self-assembly.[29-33] A partially or entirely crystalline internal structure also breaks the continuous central symmetry (rotational invariance) and brings about intrinsic optical anisotropy that can take over the role of aspect ratio.[34-36] Therefore, depolarized scattering was used to follow the growth of lamellar grains in a block copolymer,[37] and identify the onset of crystallization of biological macromolecules.[38-41] A new situation where DDLS also performs better than competing techniques[22, 42-43] is found in nearly all nanotoxicological assays, and concerns particles dispersed in biological and physiological media, for testing cellular responses.[44]

The importance of anisotropy and depolarized scattering however goes beyond particle sizing. Anisotropy offers the possibility of constructing nano- and meso-structures via self-assembly with an unprecedented variety,[45-48] and particles with novel surface properties.[49-50] The so-called patchy particles feature interactions whose range and directions are controlled, and they provide the ability to place and orientate themselves into ordered and hierarchical structures by spontaneously assembling elementary blocks from solution, which is a potentially straightforward and low-cost approach.[51-56] Shape anisotropy also exhibits unexpected[57] and applicable[58] dynamic behavior in soft-confinement, and the enhanced sensitivity of DDLS towards Brownian dynamics[21-22] is found to be useful in exploring inter-particle interactions,[59-61] the influence of confinement,[62-63] and the viscoelastic properties of soft matrices, such as gels.[64-67]

Accuracy and Precision of the Coefficient of Variation

The term "accuracy" refers to the closeness of an estimate to the true value (or population value), and the term "precision" refers to the degree of agreement in a series of estimates.

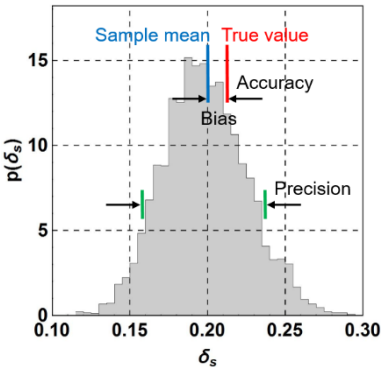

Figure SI1. a) A graph showing the plot of the sampling distribution of the coefficient of variation, illustrating the terms "accuracy" and "precision". The smaller the bias between the true value and sample mean, the smaller the range of accuracy. The narrower the distribution of the sample estimate, the smaller the range of precision.

We tested the validity of Equation 9 against independent computational experiments. We randomly drew s elements from a population of normally distributed values ($\delta = \sigma/\mu$) and computed the sample coefficient of variation ($\delta_s = \sigma_s/\mu_s$). The details of generating pseudo-random numbers is given elsewhere.[68] To construct sufficiently accurate distributions at each value of s we tested, we repeated each draw 10^3 times. Figure SI2 shows a sample of Gaussian variables ($s = 10^3$) and its estimated PDF.

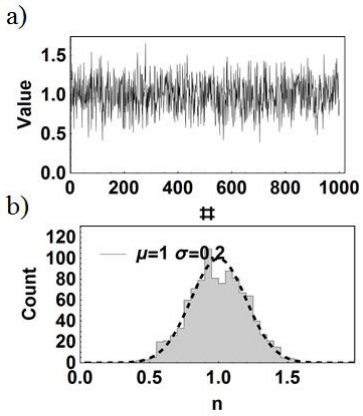

Figure SI2 a) Plot showing a sample containing 1000 elements, and b) its probability density function (PDF) estimated via counting. The dashed line is the unadjusted Gaussian curve corresponding to μ and σ.

Figure SI 3 shows the results of the computational experiments and the curves given independently by Equation 5.

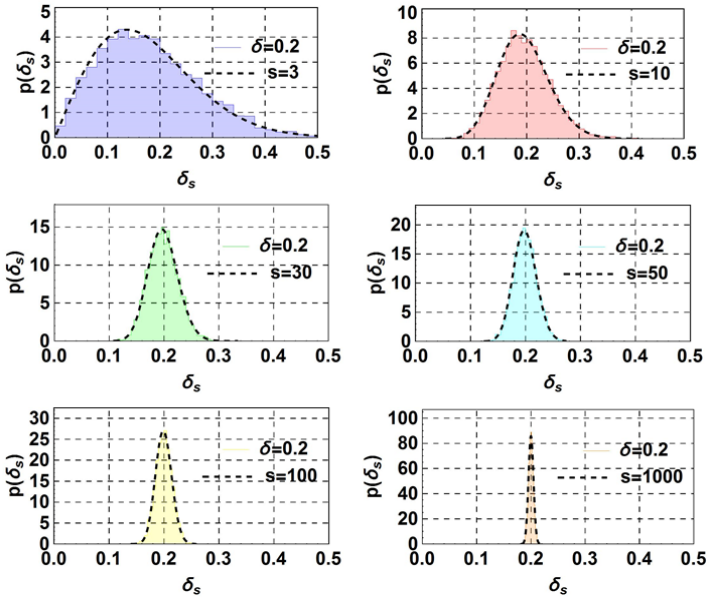

Figure SI3. The PDFs of the sample coefficient of variation (δ_s) estimated from computational experiments at different sample sizes (s = 3, 10, 30, 50, 100, and 1000). The dashed lines are the theoretical predictions given by Equation 5.

The agreement between the two data sets was excellent, and therefore, we were confident in applying it further to estimate the expectable accuracy and precisions as a

function of the sample size. The accuracy and precision intimately relate to the sample mean and variance (Figure SI1), which are defined as:

(1-SI) $\text{Mean}\ \delta_s = \int_0^1 \delta_s\, p(\delta, s; \delta_s)\, d\delta_s$

(2-SI) $\text{Var}\ \delta_s = \int_0^1 (\delta_s - \text{Mean}\ \delta_s)^2\, p(\delta, s; \delta_s)\, d\delta_s$.

After evaluating Equation 1 and 2, we obtained that

(3-SI) $\text{Mean}\ \delta_s \cong \sqrt{1 - \frac{1}{2s}}\ \delta$

(4-SI) $\text{Var}\ \delta_s \cong \frac{1}{2s}\delta^2$.

As the sample size increases, the width of the sample PDFs becomes narrower, while the mean value display a less critical dependence.

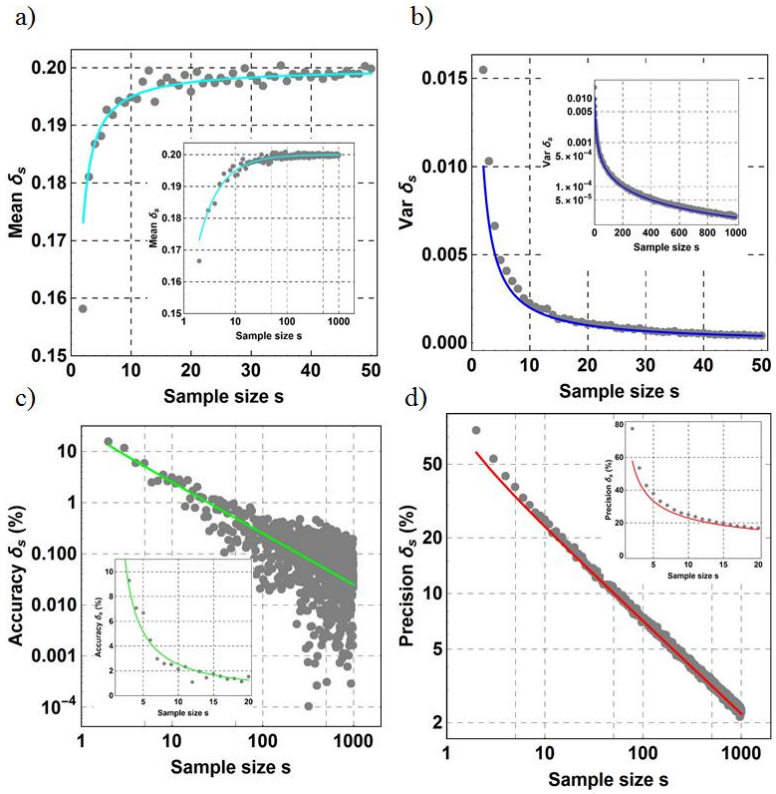

Figure SI4. a) The comparison between theory and computational experiments. The expected sample mean and b) sample variance as a function of the sample size. The solid line are the theoretical curves given by Equation 3-SI and 4-SI, respectively. The

insets show the results on an extended range. c) The expected ranges of accuracy and d) precision of the sample mean as a function of the sample size. The insets show the results on the early narrow range. The solid lines are the theoretical curves given by Equation 5-SI and 6-SI, respectively.

Figure SI4a and b display the results of computational experiments in which the sample mean and sample variance were determined as a function the sample size. Finally, we calculated the ranges of accuracy and precision of determining the sample mean (Figure SI4c and d)

$$\text{(5-SI)} \qquad \text{Accuracy } \delta_s \equiv \frac{|\text{Mean } \delta_s - \delta|}{\delta} \cong \sqrt{1 - \frac{1}{2s}} - 1$$

$$\text{(6-SI)} \qquad \text{Precision } \delta_s \equiv \frac{\sqrt{\text{Var } \delta_s}}{\text{Mean } \delta_s} \cong \frac{1}{\sqrt{2s-1}}.$$

The agreement between theory and the computational experiment was excellent.

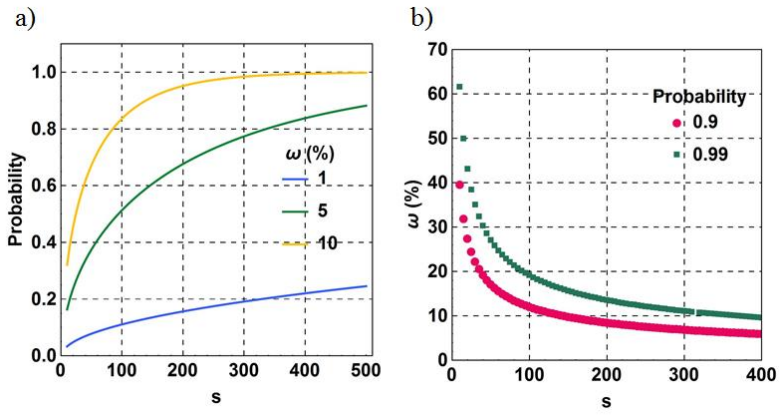

Figure SI5. The relationship between bias and probability at different ranges of accuracy as a function of the size of one single sample. a) Graph showing the probability as a function sample size at given range of expected accuracy. b) Graph showing the expectable accuracy with a given probability as a function of the sample size.

There are however alternative ways to express the expected outcome of randomness. Relying on Equation 5, we can determine the probability (P) that the bias of the mean of *one single sample* of s elements is within e.g. 10%, that is, the range of accuracy is within 10%. This means that the difference given by $\Delta\delta = \delta_s - \delta$ falls within the interval of $\delta \pm 0.1 \cdot \delta$, and $|\Delta\delta| \leq 0.1 \cdot \delta$. We estimate this probability by

(7-SI) $$P(\delta, \omega) = \int_{\delta-\omega\cdot\delta}^{\delta+\omega\cdot\delta} \delta_s \, p(\delta, s; \delta_s) \, d\delta_s,$$

where ω defines the percentage, for example, $\omega = 0.1$ corresponds to 10% accuracy.

Multiple Scattering

For larger particles with a relatively high scattering contrast (for silica the refractive index at 660 nm is ~1.45), multiple scattering may limit the system to very low concentrations. When multiple scattering is significant, the correlation function exhibits a faster decay and shows the features of increased polydispersity. An effective solution of this problem is to suppress multiple scattering in dynamic light scattering experiments using cross-correlation schemes.[69-71] This technique is available to us—but only for addressing conventional DLS where one can only probe the polarized component of the scattered light. Figure S3 shows PCS spectra recorded for two samples (SiO_2-B and D particles). If multiple scattering is significant, we expect that the intensity auto-correlation function recorded by the standard scheme (PCS) decays faster than the one recorded in the 3D-cross correlation setup (3D-Cross PCS) using two beams intersecting one another inside the sample. If multiple scattering is negligible, we expect that there is no practical difference between the decay of the PCS spectra. These results confirms that contributions from multiple scattering was negligible.

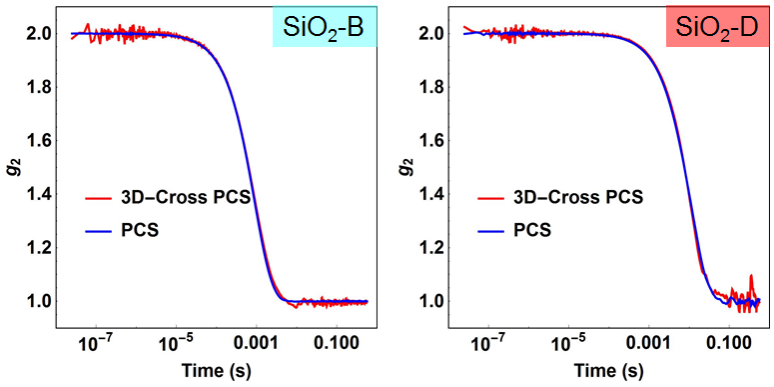

Figure S3. Conventional DLS intensity auto-correlation functions recorded in standard scheme (PCS) and 3D-cross correlation scheme (3D-Cross PCS).[69]

The Influence of Sedimentation of the Particles

Given that the scattering plane and the vector of gravity were perpendicular to each another—as it is the case for most light scattering instrument—, the settling velocity does not shift the phase of the scattered light.[72] Therefore, the dynamics of sedimentation—during e.g. 300s, the distance a particle of 400 nm cover is approx. 40 µm, assuming a mass density of 2.65 g/cm³—is not present in the fluctuations of the speckle pattern, and accordingly, it does not affect either the correlation function or the photon count statistics. If particles were highly polydisperse, settling could fractionate the sample during a long measurement, and the ensemble of the particles we observed in a given scattering volume could significantly change.

References

1. Martchenko, I.; Dietsch, H.; Moitzi, C.; Schurtenberger, P., Hydrodynamic Properties of Magnetic Nanoparticles with Tunable Shape Anisotropy: Prediction and Experimental Verification. *J. Phys. Chem. B* **2011**, *115*, 14838-14845.

2. Rodríguez-Fernández, J.; Pérez−Juste, J.; Liz−Marzán, L. M.; Lang, P. R., Dynamic Light Scattering of Short Au Rods with Low Aspect Ratios. *J. Phys. Chem. C* **2007**, *111*, 5020-5025.

3. Glidden, M.; Muschol, M., Characterizing Gold Nanorods in Solution Using Depolarized Dynamic Light Scattering. *J. Phys. Chem. C* **2012**, *116*, 8128-8137.

4. van der Zande, B. M. I.; Dhont, J. K. G.; Böhmer, M. R.; Philipse, A. P., Colloidal Dispersions of Gold Rods Characterized by Dynamic Light Scattering and Electrophoresis. *Langmuir* **2000**, *16*, 459-464.

5. Lehner, D.; Lindner, H.; Glatter, O., Determination of the Translational and Rotational Diffusion Coefficients of Rodlike Particles Using Depolarized Dynamic Light Scattering. *Langmuir* **2000**, *16*, 1689-1695.

6. Alam, S.; Mukhopadhyay, A., Translational and Rotational Diffusions of Nanorods within Semidilute and Entangled Polymer Solutions. *Macromolecules* **2014**, *47*, 6919-6924.

7. Matsuoka, H.; Morikawa, H.; Yamaoka, H., Rotational Diffusion of Ellipsoidal Latex Particles in Dispersion as Studied by Depolarized Dynamic Light Scattering. *Colloids Surf., A* **1996**, *109*, 137-145.

8. Petekidis, G.; Vlassopoulos, D.; Fytas, G.; Rülkens, R.; Wegner, G.; Fleischer, G., Diffusion Dynamics of Hairy-Rod Polymers in Concentrated Solutions. *Macromolecules* **1998**, *31*, 6139-6147.

9. Stadele, V.; Gasser, U.; Dietsch, H., Ellipsoidal Hybrid Magnetic Microgel Particles with Thermally Tunable Aspect Ratios. *Soft Matter* **2012**, *8*, 4427-4431.

10. De Souza Lima, M. M.; Wong, J. T.; Paillet, M.; Borsali, R.; Pecora, R., Translational and Rotational Dynamics of Rodlike Cellulose Whiskers. *Langmuir* **2003**, *19*, 24-29.

11. Lee, H. S.; Yun, C. H., Translational and Rotational Diffusions of Multiwalled Carbon Nanotubes with Static Bending. *J. Phys. Chem. C* **2008**, *112*, 10653-10658.

12. Shetty, A. M.; Wilkins, G. M. H.; Nanda, J.; Solomon, M. J., Multiangle Depolarized Dynamic Light Scattering of Short Functionalized Single-Walled Carbon Nanotubes. *J. Phys. Chem. C* **2009**, *113*, 7129-7133.

13. Eitoku, T.; Tange, M.; Kato, H.; Okazaki, T., Depolarized Dynamic Light Scattering Study of Multi-Walled Carbon Nanotubes in Solution. *Materials Express* **2013**, *3*, 37-42.

14. Badaire, S.; Poulin, P.; Maugey, M.; Zakri, C., In Situ Measurements of Nanotube Dimensions in Suspensions by Depolarized Dynamic Light Scattering. *Langmuir* **2004**, *20*, 10367-10370.

15. Hiroi, T.; Ata, S.; Shibayama, M., Transitions of Aggregation States for Concentrated Carbon Nanotube Dispersion. *J. Phys. Chem. C* **2016**, *120*, 5776-5782.

16. Tetsuya, S.; Tatsuro, M.; ShinobuKoda; Hiroyasu, N., Depolarized Light Scattering of Liquid Crystals with Addition of Carbon Tetrachloride in the Isotropic Phase. *Jpn. J. Appl. Phys.* **1999**, *38*, 2059.

17. Sánchez-Miranda, M. J.; Sarmiento-Gómez, E.; Arauz-Lara, J. L., Brownian Motion of Optically Anisotropic Spherical Particles in Polymeric Suspensions. *Eur. Phys. J. E* **2015**, *38*, 1-6.

18. Haghighi, M.; Plum, M. A.; Gantzounis, G.; Butt, H.-J.; Steffen, W.; Fytas, G., Plasmon-Enhanced Dynamic Depolarized Light Scattering. *J. Phys. Chem. C* **2013**, *117*, 8411-8419.

19. Zimbone, M.; Messina, E.; Compagnini, G.; Fragalà, M. E.; Calcagno, L., Resonant Depolarized Dynamic Light Scattering of Silver Nanoplatelets. *J. Nanopart. Res.* **2015**, *17*, 1-8.

20. Koch, A. H. R.; Lévêque, G.; Harms, S.; Jaskiewicz, K.; Bernhardt, M.; Henkel, A.; Sönnichsen, C.; Landfester, K.; Fytas, G., Surface Asymmetry of Coated Spherical Nanoparticles. *Nano Letters* **2014**, *14*, 4138-4144.

21. Balog, S.; Rodriguez-Lorenzo, L.; Monnier, C. A.; Michen, B.; Obiols-Rabasa, M.; Casal-Dujat, L.; Rothen-Rutishauser, B.; Petri-Fink, A.; Schurtenberger, P., Dynamic Depolarized Light Scattering of Small Round Plasmonic Nanoparticles: When Imperfection Is Only Perfect. *J. Phys. Chem. C* **2014**, *118*, 17968-17974.

22. Geers, C.; Rodriguez-Lorenzo, L.; Andreas Urban, D.; Kinnear, C.; Petri-Fink, A.; Balog, S., A New Angle on Dynamic Depolarized Light Scattering: Number-Averaged Size Distribution of Nanoparticles in Focus. *Nanoscale* **2016**, *8*, 15813-15821.

23. Antoniou, E.; Voudouris, P.; Larsen, A.; Loppinet, B.; Vlassopoulos, D.; Pastoriza-Santos, I.; Liz-Marzán, L. M., Static and Dynamic Plasmon-Enhanced Light Scattering from Dispersions of Polymer-Grafted Silver Nanoprisms in the Bulk and near Solid Surfaces. *J. Phys. Chem. C* **2012**, *116*, 3888-3896.

24. Zimbone, M.; Calcagno, L.; Messina, G.; Baeri, P.; Compagnini, G., Dynamic Light Scattering and Uv–Vis Spectroscopy of Gold Nanoparticles Solution. *Mater. Lett.* **2011**, *65*, 2906-2909.

25. Voets, I. K.; Fokkink, R.; Hellweg, T.; King, S. M.; Waard, P. d.; Keizer, A. d.; Cohen Stuart, M. A., Spontaneous Symmetry Breaking: Formation of Janus Micelles. *Soft Matter* **2009**, *5*, 999-1005.

26. Hoffmann, M.; Lu, Y.; Schrinner, M.; Ballauff, M.; Harnau, L., Dumbbell-Shaped Polyelectrolyte Brushes Studied by Depolarized Dynamic Light Scattering. *J. Phys. Chem. B* **2008**, *112*, 14843-14850.

27. Hoffmann, M.; Siebenburger, M.; Harnau, L.; Hund, M.; Hanske, C.; Lu, Y.; Wagner, C. S.; Drechsler, M.; Ballauff, M., Thermoresponsive Colloidal Molecules. *Soft Matter* **2010**, *6*, 1125-1128.

28. Chu, F., et al., Synthesis and Characterization of Monodisperse Thermosensitive Dumbbell-Shaped Microgels. *Macromol. Rapid Commun.* **2012**, *33*, 1042-1048.

29. Vailati, A.; Asnaghi, D.; Giglio, M.; Piazza, R., Depolarized Dynamic Light Scattering from Optically Anisotropic Reaction-Limited Aggregates. *Phys. Rev. E* **1993**, *48*, R2358-R2361.

30. Hoffmann, M.; Wagner, C. S.; Harnau, L.; Wittemann, A., 3d Brownian Diffusion of Submicron-Sized Particle Clusters. *ACS Nano* **2009**, *3*, 3326-3334.

31. Zimbone, M.; Musumeci, P.; Baeri, P.; Messina, E.; Boninelli, S.; Compagnini, G.; Calcagno, L., Rotational Dynamics of Gold Nanoparticle Chains in Water Solution. *J. Nanopart. Res.* **2012**, *14*, 1-11.

32. Hirsch, V.; Kinnear, C.; Rodriguez-Lorenzo, L.; Monnier, C. A.; Rothen-Rutishauser, B.; Balog, S.; Petri-Fink, A., In Vitro Dosimetry of Agglomerates. *Nanoscale* **2014**, *6*, 7325-31.

33. Guo, R.-H.; Hua, C.-C.; Lin, P.-C.; Wang, T.-Y.; Chen, S.-A., Mesoscale Aggregation Properties of C60 in Toluene and Chlorobenzene. *Soft Matter* **2016**, *12*, 6300-6311.

34. Degiorgio, V.; Piazza, R.; Bellini, T., Static and Dynamic Light Scattering Study of Fluorinated Polymer Colloids with a Crystalline Internal Structure. *Adv. Colloid Interface Sci.* **1994**, *48*, 61-91.

35. Escobedo-Sánchez, M. A.; De la Cruz-Burelo, H. A.; Arauz-Lara, J. L.; Haro-Pérez, C.; Rojas-Ochoa, L. F., Study of Translational and Rotational Dynamics of Birefringent Colloidal Particles by Depolarized Light Scattering in the Far- and near-Field Regimes. *J. Chem. Phys.* **2015**, *143*, 044902.

36. Koenderink, G. H.; Sacanna, S.; Aarts, D. G.; Philipse, A. P., Rotational and Translational Diffusion of Fluorocarbon Tracer Spheres in Semidilute Xanthan Solutions. *Phys. Rev. E* **2004**, *69*, 021804.

37. Wang, X.; Thelen, J. L.; Teran, A. A.; Chintapalli, M.; Nakamura, I.; Wang, Z.-G.; Newstein, M. C.; Balsara, N. P.; Garetz, B. A., Evolution of Grain Structure During Disorder-to-Order Transitions in a Block Copolymer/Salt Mixture Studied by Depolarized Light Scattering. *Macromolecules* **2014**, *47*, 5784-5792.

38. Chayen, N.; Dieckmann, M.; Dierks, K.; Fromme, P., Size and Shape Determination of Proteins in Solution by a Noninvasive Depolarized Dynamic Light Scattering Instrument. *Ann. N.Y. Acad. Sci.* **2004**, *1027*, 20-27.

39. Schubert, R.; Meyer, A.; Dierks, K.; Kapis, S.; Reimer, R.; Einspahr, H.; Perbandt, M.; Betzel, C., Reliably Distinguishing Protein Nanocrystals from Amorphous Precipitate by Means of Depolarized Dynamic Light Scattering. *J. Appl. Crystallogr.* **2015**, *48*, 1476-1484.

40. Cipolla, D., et al., Formation of Drug Nanocrystals under Nanoconfinement Afforded by Liposomes. *RSC Advances* **2016**, *6*, 6223-6233.

41. Maes, D.; Vorontsova, M. A.; Potenza, M. A. C.; Sanvito, T.; Sleutel, M.; Giglio, M.; Vekilov, P. G., Do Protein Crystals Nucleate within Dense Liquid Clusters? *Acta Crystallogr., Sect. F* **2015**, *71*, 815-822.

42. Urban, D. A.; Rodriguez-Lorenzo, L.; Balog, S.; Kinnear, C.; Rothen-Rutishauser, B.; Petri-Fink, A., Plasmonic Nanoparticles and Their Characterization in Physiological Fluids. *Colloids Surf., B* **2016**, *137*, 39-49.

43. Balog, S.; Rodriguez-Lorenzo, L.; Monnier, C. A.; Obiols-Rabasa, M.; Rothen-Rutishauser, B.; Schurtenberger, P.; Petri-Fink, A., Characterizing Nanoparticles in Complex Biological Media and Physiological Fluids with Depolarized Dynamic Light Scattering. *Nanoscale* **2015**, *7*, 5991-7.

44. Moore, T. L.; Rodriguez-Lorenzo, L.; Hirsch, V.; Balog, S.; Urban, D.; Jud, C.; Rothen-Rutishauser, B.; Lattuada, M.; Petri-Fink, A., Nanoparticle Colloidal Stability in Cell Culture Media and Impact on Cellular Interactions. *Chem. Soc. Rev.* **2015**, *44*, 6287-6305.

45. Li, F.; Josephson, D. P.; Stein, A., Colloidal Assembly: The Road from Particles to Colloidal Molecules and Crystals. *Angew. Chem. Int. Ed.* **2011**, *50*, 360-388.

46. Zhang; Glotzer, S. C., Self-Assembly of Patchy Particles. *Nano Letters* **2004**, *4*, 1407-1413.

47. Glotzer, S. C.; Solomon, M. J., Anisotropy of Building Blocks and Their Assembly into Complex Structures. *Nat Mater* **2007**, *6*, 557-562.

48. Plüisch, C. S.; Wittemann, A., Shape-Tailored Polymer Colloids on the Road to Become Structural Motifs for Hierarchically Organized Materials. *Macromol. Rapid Commun.* **2013**, *34*, 1798-1814.

49. Devries, G. A.; Brunnbauer, M.; Hu, Y.; Jackson, A. M.; Long, B.; Neltner, B. T.; Uzun, O.; Wunsch, B. H.; Stellacci, F., Divalent Metal Nanoparticles. *Science* **2007**, *315*, 358-61.

50. Jackson, A. M.; Myerson, J. W.; Stellacci, F., Spontaneous Assembly of Subnanometre-Ordered Domains in the Ligand Shell of Monolayer-Protected Nanoparticles. *Nat Mater* **2004**, *3*, 330-336.

51. Renna, L. A.; Boyle, C. J.; Gehan, T. S.; Venkataraman, D., Polymer Nanoparticle Assemblies: A Versatile Route to Functional Mesostructures. *Macromolecules* **2015**, *48*, 6353-6368.

52. Wang, Y.; Wang, Y.; Breed, D. R.; Manoharan, V. N.; Feng, L.; Hollingsworth, A. D.; Weck, M.; Pine, D. J., Colloids with Valence and Specific Directional Bonding. *Nature* **2012**, *491*, 51-55.

53. Akcora, P., et al., Anisotropic Self-Assembly of Spherical Polymer-Grafted Nanoparticles. *Nat Mater* **2009**, *8*, 354-359.

54. Schreiber, R.; Santiago, I.; Ardavan, A.; Turberfield, A. J., Ordering Gold Nanoparticles with DNA Origami Nanoflowers. *ACS Nano* **2016**, *10*, 7303-7306.

55. Choueiri, R. M., et al., Surface Patterning of Nanoparticles with Polymer Patches. *Nature* **2016**, *538*, 79-83.

56. Boles, M. A.; Engel, M.; Talapin, D. V., Self-Assembly of Colloidal Nanocrystals: From Intricate Structures to Functional Materials. *Chem. Rev.* **2016**.

57. Choi, J.; Cargnello, M.; Murray, C. B.; Clarke, N.; Winey, K. I.; Composto, R. J., Fast Nanorod Diffusion through Entangled Polymer Melts. *ACS Macro Letters* **2015**, *4*, 952-956.

58. Chen, K.; Xu, J.; Luft, J. C.; Tian, S.; Raval, J. S.; DeSimone, J. M., Design of Asymmetric Particles Containing a Charged Interior and a Neutral Surface Charge: Comparative Study on in Vivo Circulation of Polyelectrolyte Microgels. *JACS* **2014**, *136*, 9947-9952.

59. Rallison, J. M.; Hinch, E. J., The Effect of Particle Interactions on Dynamic Light-Scattering from a Dilute Suspension. *J Fluid Mech* **1986**, *167*, 131-168.

60. Piazza, R.; Degiorgio, V., Rotational and Translational Self-Diffusion Coefficients of Interacting Brownian Spheres. *J. Phys.: Condens. Matter* **1993**, *5*, B173.

61. Degiorgio, V. V.; Piazza, R.; Jones, R. B., Rotational Diffusion in Concentrated Colloidal Dispersions of Hard Spheres. *Phys. Rev. E* **1995**, *52*, 2707-2717.

62. Haghighi, M.; Tahir, M. N.; Tremel, W.; Butt, H.-J.; Steffen, W., Translational and Rotational Diffusion of Gold Nanorods near a Wall. *J. Chem. Phys.* **2013**, *139*, 064710.

63. Lisicki, M.; Cichocki, B.; Rogers, S. A.; Dhont, J. K. G.; Lang, P. R., Translational and Rotational near-Wall Diffusion of Spherical Colloids Studied by Evanescent Wave Scattering. *Soft Matter* **2014**, *10*, 4312-4323.

64. Sara, J.-F.; Erika, E.; Gerard, H. W.; Daniel, B., Ageing Dynamics of Translational and Rotational Diffusion in a Colloidal Glass. *J. Phys.: Condens. Matter* **2004**, *16*, L471.

65. Jabbari-Farouji, S.; Wegdam, G. H.; Bonn, D., Aging of Rotational Diffusion in Colloidal Gels and Glasses. *Phys. Rev. E* **2012**, *86*, 041401.

66. Chen, S.; Kraus, T., Nanorod-Depolarized Dynamic Light Scattering in a Gelling Liquid. *J. Phys. Chem. C* **2012**, *116*, 16766-16775.

67. Bica, C. I. D.; Borsali, R.; Rochas, C.; Geissler, E., Dynamics of Cellulose Whiskers Spatially Trapped in Agarose Hydrogels. *Macromolecules* **2006**, *39*, 3622-3627.

68. Random Number Generation. In Wolfram Language & System Documentation Center.

69. Urban, C.; Schurtenberger, P., Characterization of Turbid Colloidal Suspensions Using Light Scattering Techniques Combined with Cross-Correlation Methods. *J. Colloid Interface Sci.* **1998**, *207*, 150-158.

70. Moussaïd, A.; Pusey, P. N., Multiple Scattering Suppression in Static Light Scattering by Cross-Correlation Spectroscopy. *Phys. Rev. E* **1999**, *60*, 5670-5676.

71. Pusey, P. N., Suppression of Multiple Scattering by Photon Cross-Correlation Techniques. *Curr. Opin. Colloid Interface Sci.* **1999**, *4*, 177-185.

72. Chowdhury, D. P.; Sorensen, C. M.; Taylor, T. W.; Merklin, J. F.; Lester, T. W., Application of Photon Correlation Spectroscopy to Flowing Brownian Motion Systems. *Appl. Opt.* **1984**, *23*, 4149-4154.